

Time-lapse by the numbers: elastic modeling of repeatability issues

David C. Henley*, Joe Wong, and Peter M. Manning

dhenley@ucalgary.ca

Introduction

Remote monitoring of hydrocarbon production from a formation, or CO₂ injection into a formation are increasingly important applications of reflection seismic imaging. In this application, it is important to be able to repeat a seismic survey as exactly as possible at significant time intervals after an initial ‘baseline’ survey. In addition to using the same acquisition geometry, the subsequent processing must be repeated as exactly as possible, so that each ‘monitor’ survey image differs from the initial ‘baseline’ survey only in the ‘anomalous’ zone whose actual rock properties have changed due to the extraction or injection of fluids. In order to study the detectability of a time-lapse anomaly relative to various acquisition and processing parameters, we created a series of synthetic seismic data sets from a ‘baseline’ earth model and its corresponding ‘monitor’ model, which differed only in the rock properties of an ‘anomalous’ zone in one of its layers. We used a 2D elastic modeling program written by Peter Manning and modified by Joe Wong to generate the synthetic seismic data for each model, and standard ProMAX modules to produce images from the data.

Selected modeling results

Figure 1 shows one of the ‘baseline’ models used in this study. Some features of this model include gentle undulations at the base of weathering, and large-contrast pockets of material at the surface, which cause significant statics and surface-wave scattering. Figure 2 shows the corresponding ‘monitor’ model, identical to the baseline model, except for a zone 400m long by 50m thick, in which velocity is diminished by 10% relative to the formation velocity flanking the anomaly. Figure 3 is a representative shot gather from the baseline model, with no added random noise, showing the realistic nature of the data created by the elastic modeling. Figure 4 is a CMP stack image of the simulated seismic survey over the ‘monitor’ model in Figure 2. Prior to the CMP stack, coherent noise was attenuated on the shot gathers, Gabor deconvolution was applied, and stack-power autostatics was applied to remove residual statics. Figure 5 shows the simple time-matched difference between the CMP stacks for the ‘baseline’ and ‘monitor’ models. When significant levels of bandlimited random noise ($S/N = 1$) are added to the data for both surveys, the anomaly can still be detected (Figure 6), but only if the residual statics derived for the ‘baseline’ survey are also applied to the ‘monitor’ survey. If seasonal statics differences are expected, then residual statics runs must be made independently for ‘baseline’ and ‘monitor’ surveys, but the anomaly is still detectable (Figure 7). Larger near-surface amplitudes in Figure 7 are likely due to the differences in the two statics solutions. Figure 8 shows the comparable result when raypath interferometry is used on both surveys to correct for statics.

Comments

Elastic modeling can be used to generate realistic synthetic seismic data for testing the sensitivity of acquisition and processing strategies and parameters relative to the detectability of a prospective rock-properties anomaly. Future work will explore the effects of various mismatches between datasets, such as missing data and variable trace amplitudes, as well as other comparison techniques like matched filtering.

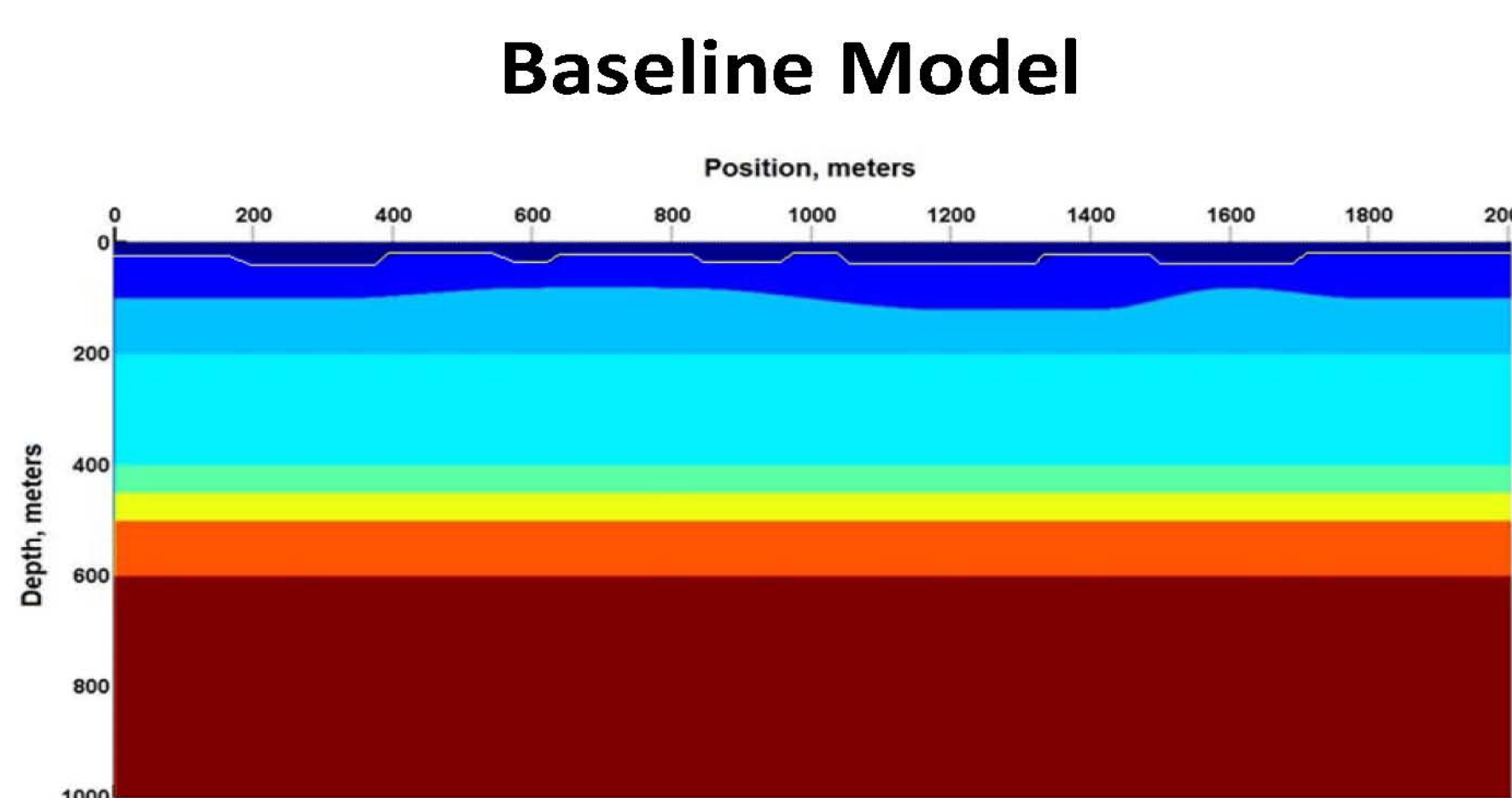


FIG. 1. Illustration of a ‘baseline’ earth model provided as input to the 2D elastic modeling program. Note undulating base of weathering layer, as well as significant ‘statics’ anomalies at the surface

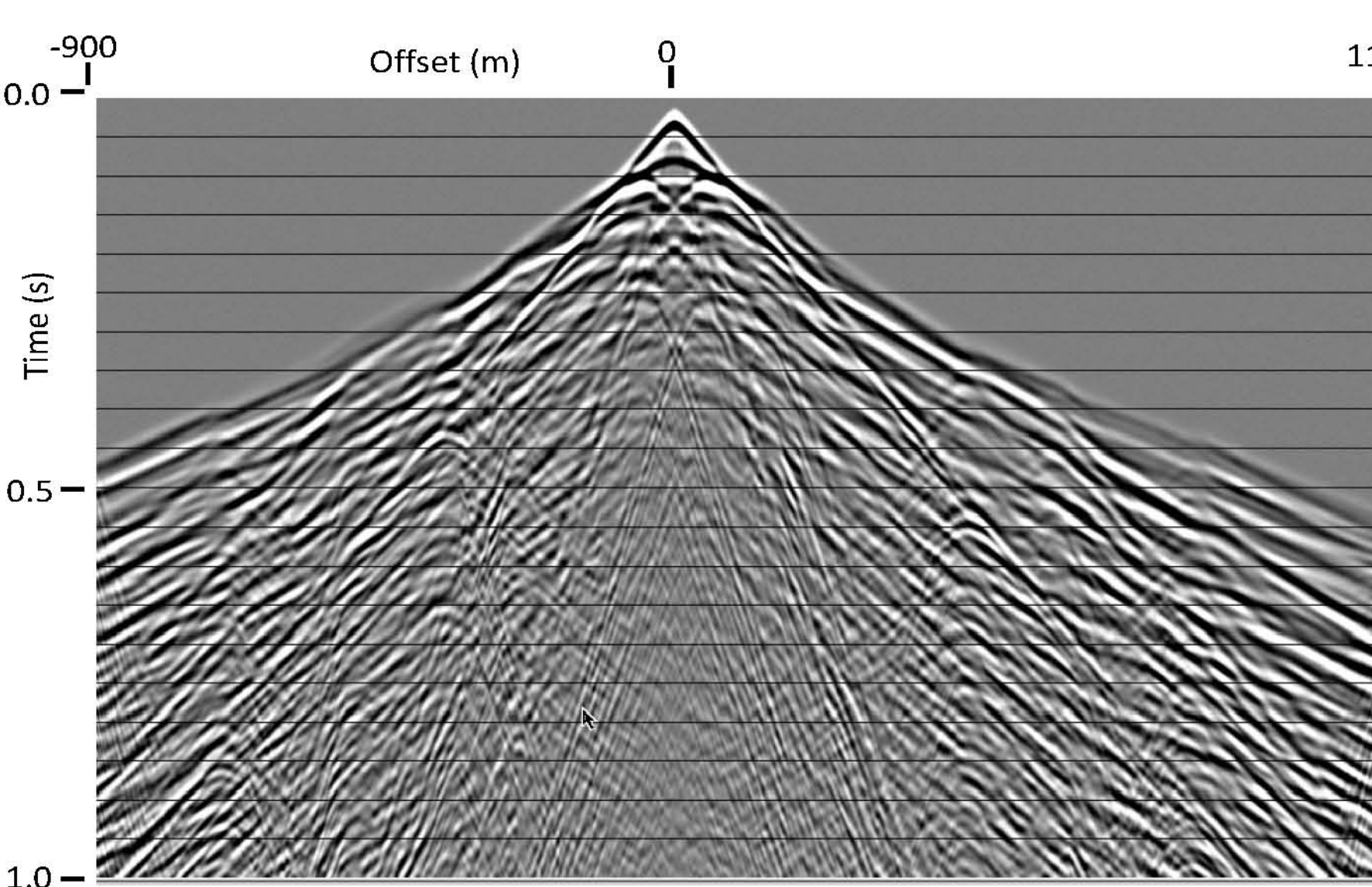


FIG. 3. Example of a shot gather generated by 2D elastic modeling near the centre of the ‘baseline’ model in Figure 1. The surface waves and scattered waves thoroughly mask any reflections.

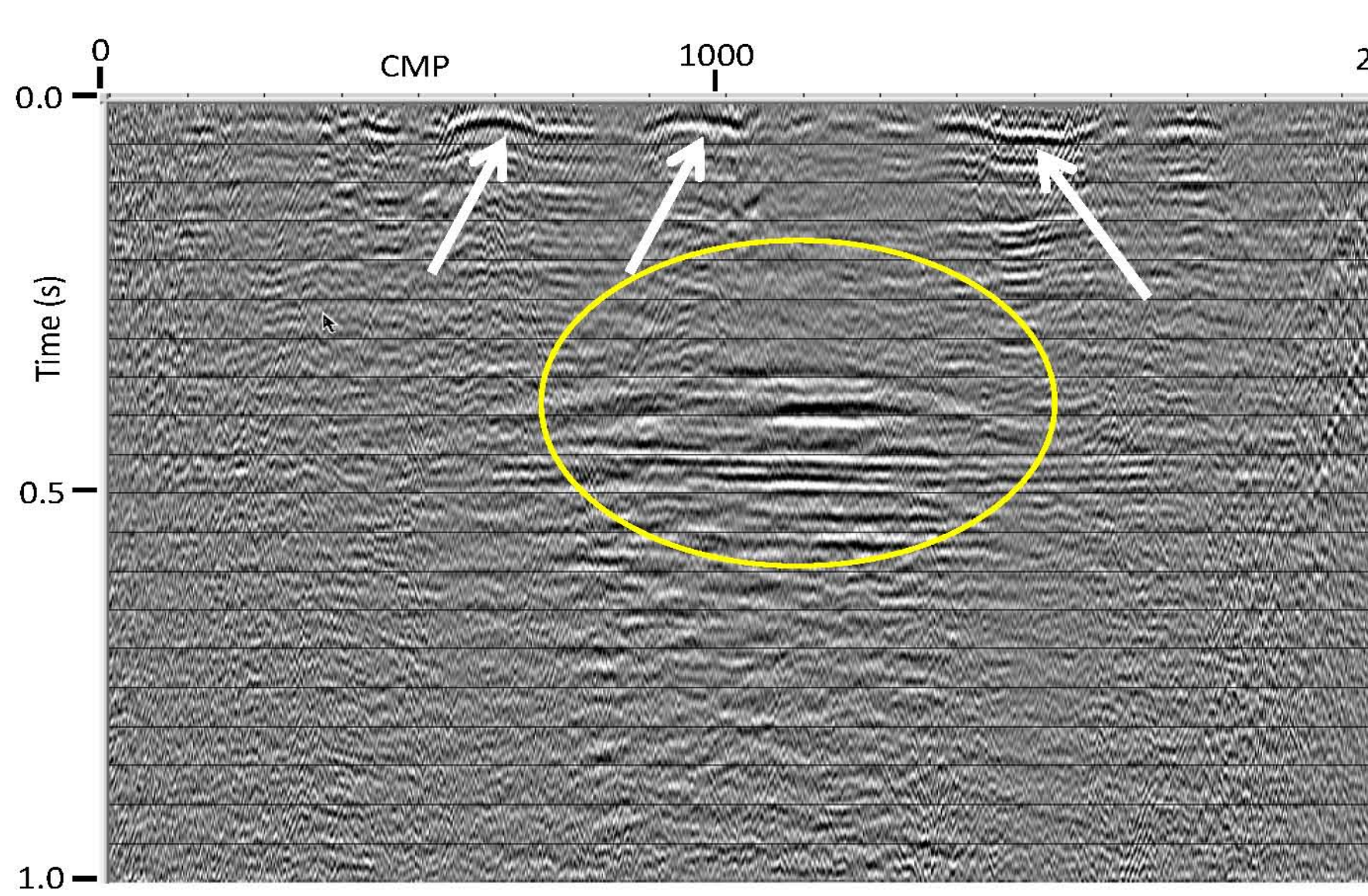


FIG. 4. CMP stack of 2D elastic model data for the ‘monitor’ survey after coherent noise attenuation, Gabor deconvolution, and stack-power residual statics.

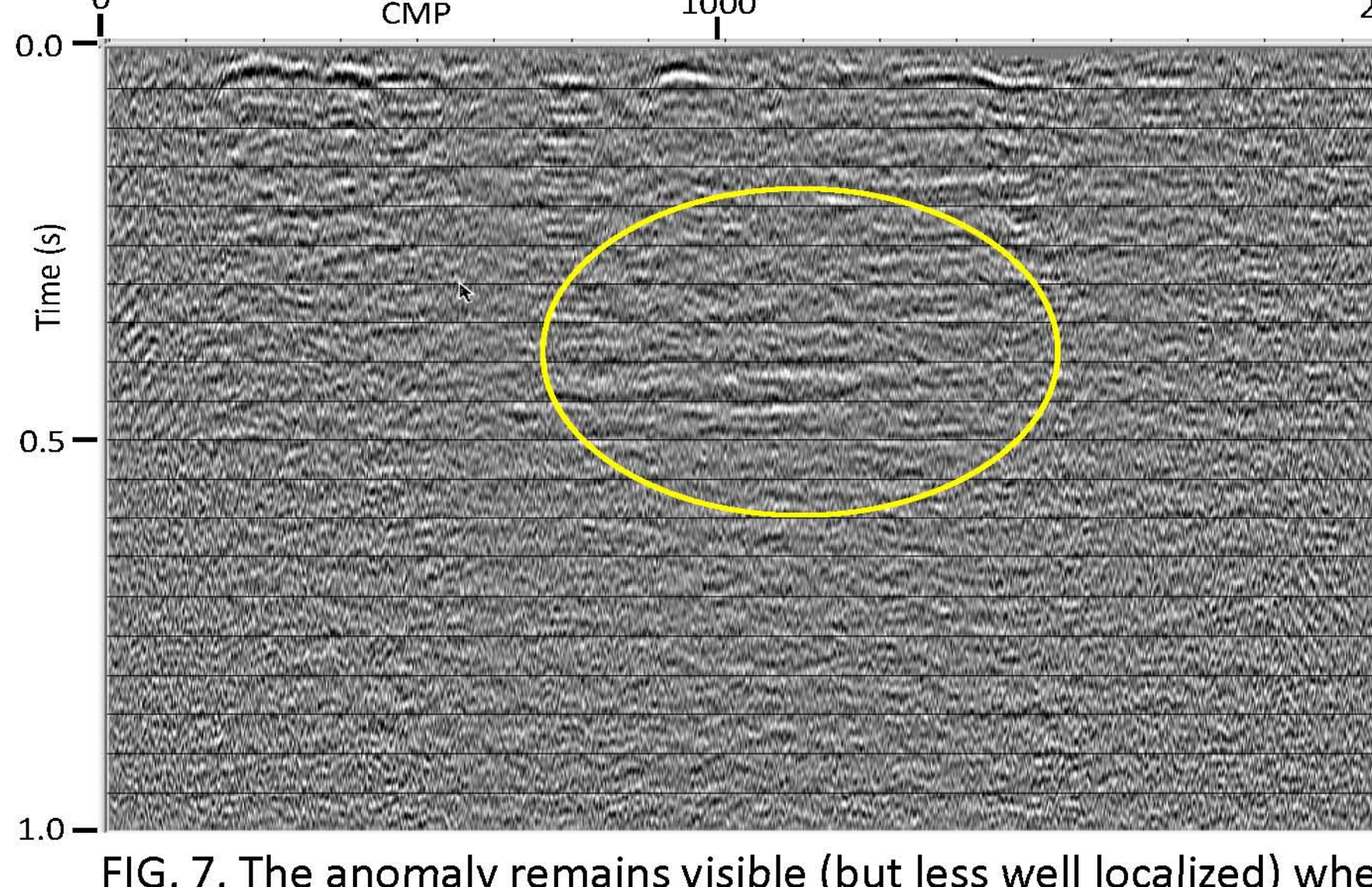


FIG. 5. Difference between CMP stacks of ‘monitor’ survey and ‘baseline’ survey. Differences between the statics solutions (run independently for the two models) lead to larger mismatch amplitudes at the surface (arrows)

FIG. 6. Even when model data sets are contaminated with high levels of random noise ($S/N=1$), the anomaly is visible, as long as the same statics are applied to both baseline and monitor surveys.

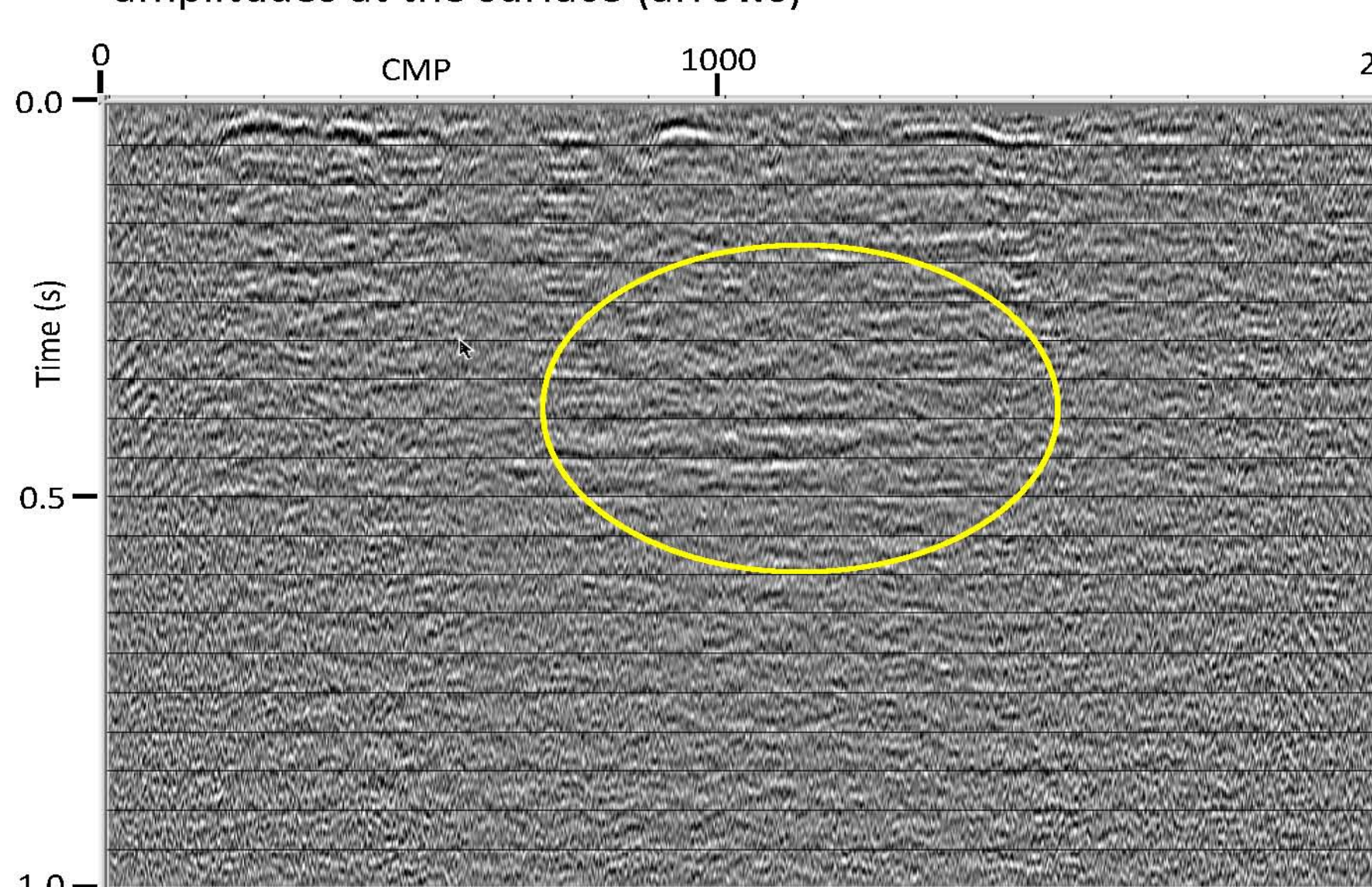


FIG. 7. The anomaly remains visible (but less well localized) when $S/N=1$ and when seasonal weathering differences are present, necessitating independent statics solutions. Larger near-surface mismatch amplitudes reflect the differences in statics.

FIG. 8. When statics are applied to both surveys with raypath interferometry, the lateral extent of the bottom of the anomaly (white arrows) is better represented, and the time mismatch of the layer beneath is more visible (red arrow).

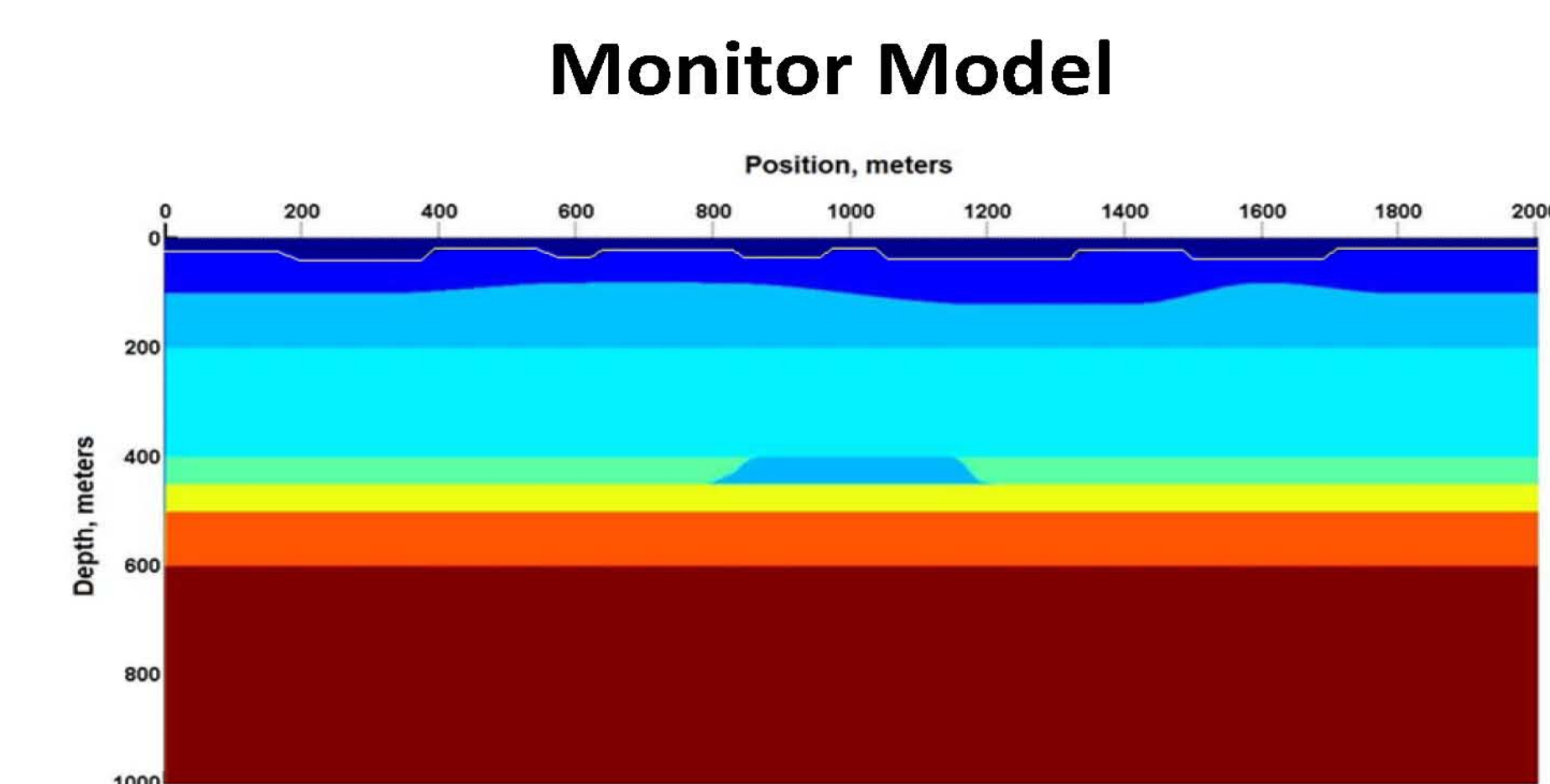


FIG. 2. Illustration of a ‘monitor’ earth model provided as input to the 2D elastic modeling program. The only difference between this model and the ‘baseline’ model in Figure 1 is the ‘anomalous’ zone in the centre of the model

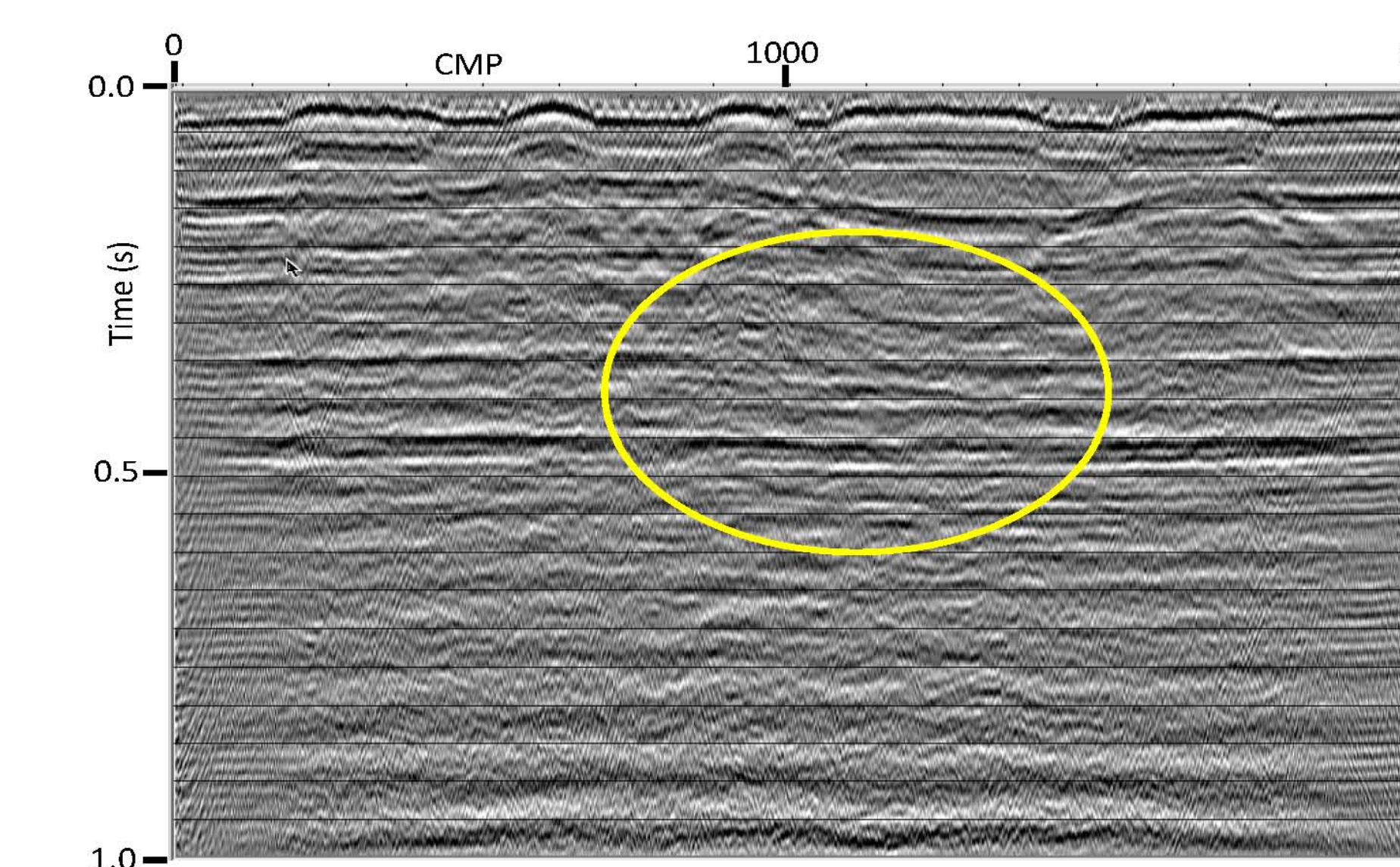


FIG. 4. CMP stack of 2D elastic model data for the ‘monitor’ survey after coherent noise attenuation, Gabor deconvolution, and stack-power residual statics.

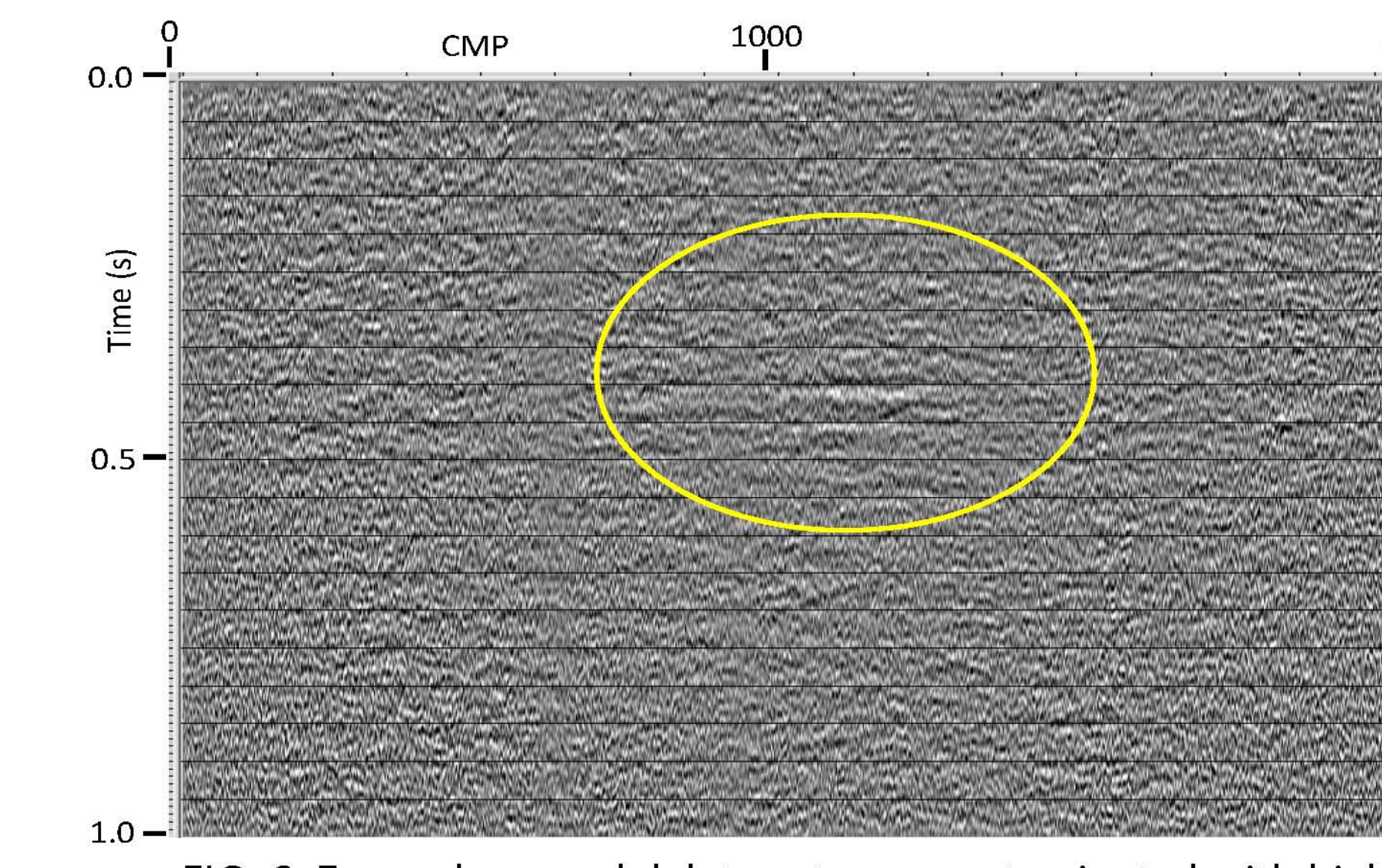


FIG. 6. Even when model data sets are contaminated with high levels of random noise ($S/N=1$), the anomaly is visible, as long as the same statics are applied to both baseline and monitor surveys.

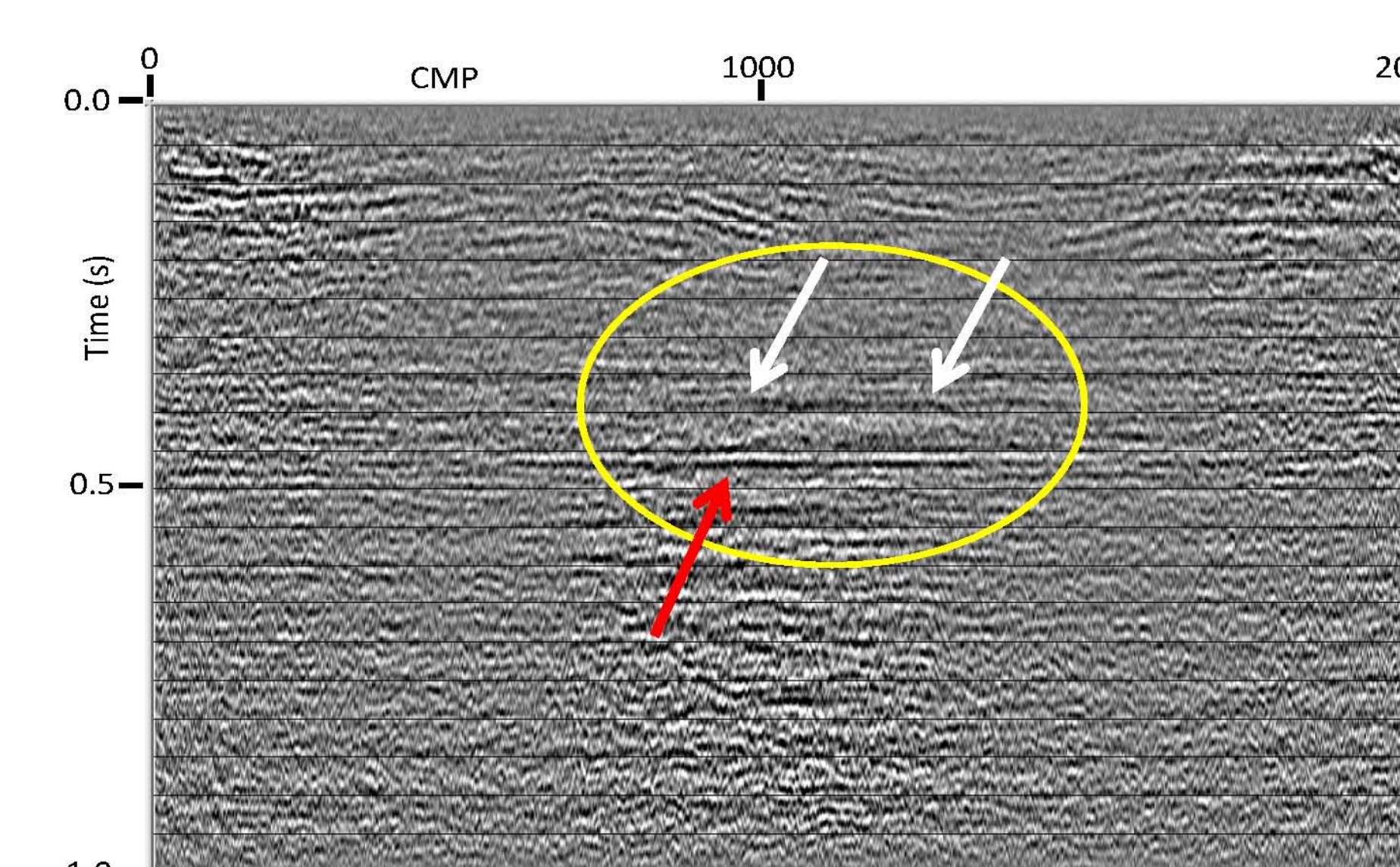


FIG. 7. The anomaly remains visible (but less well localized) when $S/N=1$ and when seasonal weathering differences are present, necessitating independent statics solutions. Larger near-surface mismatch amplitudes reflect the differences in statics.

FIG. 8. When statics are applied to both surveys with raypath interferometry, the lateral extent of the bottom of the anomaly (white arrows) is better represented, and the time mismatch of the layer beneath is more visible (red arrow).